NMR study of local magnetizations in diluted two-dimensional antiferromagnets

B. J. Dikken, C. Dekker, A. F. M. Arts, and H. W. de Wijn
Fysisch Laboratorium, Rijksuniversiteit Utrecht, Postbus 80000, 3508 TA Utrecht, The Netherlands
(Received 10 July 1985)

The local magnetizations in the diluted two-dimensional (2D) Ising antiferromagnet $K_2Co_{0.83}Zn_{0.17}F_4$ and the diluted weakly anisotropic 2D Heisenberg antiferromagnet $K_2Ni_xZn_{1-x}F_4$ with $x=0.96$ and 0.85 have been measured as a function of the temperature by tracking the ^{19}F NMR. In the diluted Ising case the decrease with temperature of the magnetization of a particular spin correlates primarily with the number of magnetic neighbors in the first shell, whereas in the Heisenberg-like systems the decrement is mainly determined by the average dilution. The relevant magnetic excitations are derived to be almost completely localized in $K_2Co_xZn_{1-x}F_4$, but spin-wave-like in $K_2Ni_xZn_{1-x}F_4$. In addition, the sublattice magnetization in pure K_2CoF_4 has been measured, and found to closely follow Onsager's result.

I. INTRODUCTION

In this paper, we report on the local magnetizations residing at individual sites in the randomly diluted two-dimensional (2D) antiferromagnets $K_2Co_xZn_{1-x}F_4$ and $K_2Ni_xZn_{1-x}F_4$ as a function of the temperature. The end members of these systems, K_2CoF_4 and K_2NiF_4, are well defined. K_2CoF_4, ordering below the Néel temperature $T_N=107.85$ K,[1] is an almost perfect 2D Ising antiferromagnet, whose sublattice magnetization closely obeys Onsager's result[2] for the quadratic $S=\frac{1}{2}$ Ising model. With a variety of techniques,[3,4] K_2NiF_4 has been shown to be a 2D Heisenberg antiferromagnet, in which a small single-ion anisotropy stabilizes the order below $T_N=97.23$ K. In both systems, as well as their diluted derivatives, the anisotropy leaves the magnetization along the tetragonal axis (c axis).

The site-to-site variation of the local magnetization in randomly diluted 2D antiferromagnets has as yet not been the subject of experimental verification. An experimental technique to distinguish between the individual sites is nuclear magnetic resonance (NMR) of adjacent ^{19}F nuclei, whose resonance frequencies directly correlate with the individual magnetic moments. The fall of these magnetizations with temperature yields information on the excitations of diluted systems, especially their extent in space and their energies. The method, which ultimately is based on a thermal property, emphasizes the low-lying excitations, although the density of states makes the weight shift out into the Brillouin zone in case the dispersion is small. This is particularly the case in the diluted Ising systems, and, for that matter, in pure K_2CoF_4, which in addition has been examined. The localization of the excitations is reflected in the way the decrements of the local magnetizations compare for various surroundings. As it turns out, the spectra are, in part because of minor modifications of the hyperfine parameters, resolved according to the number of magnetic first neighbors.

II. EXPERIMENTAL DETAILS

Single crystals of $K_2Co_xZn_{1-x}F_4$ and $K_2Ni_xZn_{1-x}F_4$, typically $10\times6\times25$ mm^3 in volume, were grown from a melt of KF, $KZnF_3$, $KCoF_3$, and $KNiF_3$ in appropriate proportions using the Czochralski pulling technique. The Zn concentrations were determined by means of atomic absorption spectroscopy. In the case of the

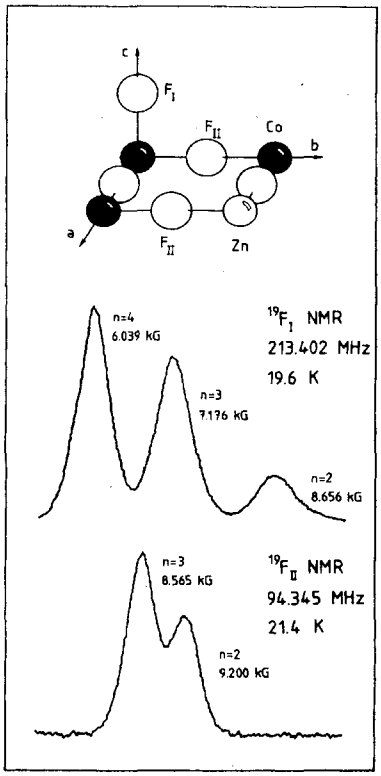

FIG. 1. Part of a quadratic layer in $K_2Co_xZn_{1-x}F_4$ with the out-of-layer F_I and the in-layer F_{II} ions indicated, and typical ^{19}F-NMR spectra in $K_2Co_{0.83}Zn_{0.17}F_4$ at low temperatures. The resonances correspond to various Co occupations n of the first shell of neighbors. Values of the fields, directed along the c axis, refer to the peak positions at the oscillator frequencies indicated.

$K_2Co_xZn_{1-x}F_4$ samples, the homogeneity of the dilution was better than 0.01 in x over the total length of the crystals. By contrast, in $K_2Ni_xZn_{1-x}F_4$ appreciable concentration fluctuations were discerned by use of a scanning electron microscope equipped with an energy-dispersive x-ray system (SEM-EDX). At $x=0.85$, for instance, x was observed to vary by 0.07 over distances of a few microns. In the experiments, samples of $K_2Co_xZn_{1-x}F_4$ with $x=1$ and 0.83, and $K_2Ni_xZn_{1-x}F_4$ with, on the average, $x=0.96$ and 0.85 were investigated.

The local magnetizations as a function of temperature below T_N may be probed with great precision by tracking the NMR frequencies of the out-of-layer $^{19}F_I$ and in-layer $^{19}F_{II}$ nuclei.[3] These nuclei resonate in the transferred hyperfine fields invoked by the adjacent magnetic ions (Fig. 1), with small dipolar contributions from further neighbors. In the diluted samples a spin-echo NMR technique was employed to determine the resonance frequencies of both the $^{19}F_I$ and the $^{19}F_{II}$. Representative spectra in $K_2Co_{0.83}Zn_{0.17}F_4$ at tempertures where the magnetization is fully developed are given in Fig. 1. In K_2CoF_4 the $^{19}F_I$ resonance frequencies were measured with cw NMR. The NMR spectrometers were equipped with a high-Q resonance circuit held at the sample temperature and tuned to a fixed frequency up to 220 MHz. Scanning was accomplished with an external magnetic field, up to 10 kG, aligned parallel to the spin orientation with an accuracy 0f 0.5°. The sample temperature, servostabilized to within 0.05 K, was measured with a calibrated carbon-glass cryoresistor.

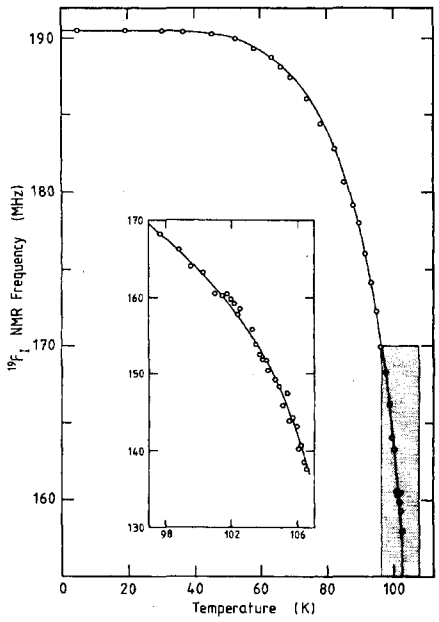

FIG. 2. Temperature dependence of the $^{19}F_I$-NMR frequency, extrapolated to zero external field, in K_2CoF_4. The solid curve represents the result of the least-squares fit of Onsager's relation, Eq. (1), to the data.

III. RESULTS AND DISCUSSION

A. Ising systems $K_2Co_xZn_{1-x}F_4$

In analyzing the NMR frequencies in $K_2Co_xZn_{1-x}F_4$, we use, because of its inherent precision (better than 1 part in 10^4), as a reference the fall with increasing temperature of the sublattice magnetization in K_2CoF_4 measured with $^{19}F_I$ NMR. We therefore discuss the results in K_2CoF_4 first. At 4.2 K, a very narrow NMR line associated with $^{19}F_I$ is found at a frequency of, extrapolated to zero field, about 190 MHz. The full width at half maximum (FWHM) is only 29 G, or 0.12 MHz. In Fig. 2, the $^{19}F_I$-NMR frequency is presented as a function of the temperature. The near constancy of this frequency up to, say, 40 K is in conformity with the Ising character of K_2CoF_4. In fact, the solid curve in Fig. 2 represents a least-squares fit to the data of Onsager's result for the magnetization $M(T)$ in the square-lattice $S=\frac{1}{2}$ Ising model,[2]

$$M(T)/M(0)=[1-\sinh^{-4}(J/k_BT)]^{1/8}, \quad (1)$$

but with allowance for the minor reduction of the transferred hyperfine parameter A_I with increasing temperature. This reduction, due to lattice vibrations, is in the temperature regime of interest adequately described by $A_I(T)=A_I(0)[1-(T/T_s)^4]$.[5] The excellent fit of Eq. (1) to the data in Fig. 2 corresponds to a zero-field zero-temperature frequency $\nu(T=0)=190.484\pm0.015$ MHz, an exchange parameter $J/k_B=-95.7\pm0.7$ K, and $T_s=275\pm15$ K. The errors represent two standard deviations and do not comprise any systematic uncertainties. For $\nu(T=0)$ the systematic errors, with inclusion of the effects of demagnetizing fields, are estimated at 0.030 MHz maximum. The excess FWHM of the $^{19}F_I$ NMR when approaching T_N from below follows the power law $(2.5\pm0.7)\times(1-T/T_N)^{-0.95\pm0.10}$ G in the regime $10^{-2}<1-T/T_N<3\times10^{-1}$. The slope, close to $-\frac{7}{8}$, and the prefactor are consistent with an inhomogeneity in the sample temperature of about 0.05 K, which is not unrealistic. A homogeneous component to the excess FWHM can, however, not be excluded because it scales with the square root of the staggered susceptibility, and thus would also exhibit an exponent $-\frac{7}{8}$.

It is noted that the adjustment of Eq. (1) to the NMR data in Fig. 2 over the entire range of temperatures overshoots the sublattice magnetization by about 0.1% at temperatures ranging from 60 to 93 K, apparently because of the finite dispersion of the excitation energies in K_2CoF_4. To better accuracy, therefore, T_N and J may be deduced by fitting Eq. (1) separately to the data near T_N and the data below about 80 K, respectively. In the former case, the staggered magnetization is, upon approximating Eq. (1) by the power law $(1-T/T_N)^{1/8}$, essentially extrapolated to zero. The result of fitting the power law to the data above 98 K is $T_N=107.9\pm0.1$ K, in excellent agreement with the result $T_N=107.85\pm0.05$ K derived from fitting $(1-T/T_N)^{2\beta}$ to neutron Bragg intensities in the critical regime.[1] A fit of Eq. (1) to the data below 80 K yields $J/k_B=-94\pm2$ K. In this context, $4|J|$ may

be regarded as an average of the excitation energy over the Brillouin zone effectively describing the drop of the magnetization. The emphasis is in that part of the zone where the density of states is maximum, i.e., close to the zone boundary. More precisely, the decrement of the sublattice magnetization equals $\sum_{\mathbf{k}}(u_{\mathbf{k}}^2+v_{\mathbf{k}}^2)n_{\mathbf{k}}$, in which $n_{\mathbf{k}}$ represents the Bose factor, and $u_{\mathbf{k}}$ and $v_{\mathbf{k}}$ denote the Bogoliubov coefficients. In case of weak dispersion, then, the experiment approximately determines

$$J \approx J_{\|}[1-\tfrac{1}{2}\gamma(J_{\perp}/J_{\|})^2(1+k_B T_m/4|J_{\|}|)] ,$$

in which $J_{\|}$ and $J_{\perp}$ are the parallel and transverse exchange constants,

$$\gamma=(4/\pi^2)\int_0^1 K((1-z^2)^{1/2})z^2dz=0.287 ,$$

and T_m denotes the maximum temperature considered in the fit. In K_2CoF_4, for which the $k=0$ energy is 18% lower than the zone-boundary energy $4|J_{\|}|$,[6] $J_{\perp}\approx 0.6J_{\|}$ in a fictitious $S=\frac{1}{2}$ spin Hamiltonian. This implies an upward correction of $|J|$ by 6% to obtain $|J_{\|}|$, resulting in $J_{\|}=-100\pm 2$ K. For comparison, a crystal-field analysis of inelastic light scattering in K_2CoF_4 has yielded the somewhat smaller value $J_{\|}=-90$ K by extrapolation from the lowest $k=0$ magnetic exciton energy.[6]

In $K_2Co_{0.83}Zn_{0.17}F_4$ the local magnetizations have been probed with NMR of $^{19}F_I$ nuclei as well as those $^{19}F_{II}$ nuclei that are situated between a Co ion and a Zn ion (Fig. 1). In the $^{19}F_I$-NMR spectra, three distinct resonances are seen, which at low temperatures are about 550 G broad (FWHM), compared with 29 G in K_2CoF_4. At 75 K, the width has risen to about 1 kG. In identifying these resonances, it is noted that all spins are fully aligned at low temperatures. The separation of the resonances at these temperatures are therefore caused solely by the local modifications of the hyperfine parameter A invoked by the substitution of Zn for Co, with inclusion of the changes of the dipolar field. These modifications depend on the immediate environment. The three $^{19}F_I$ resonances thus are to be associated with Co ions primarily according to the number of Co ions in the first shell of neighbors. The random architecture of the farther shells of course affects A as well as contributes to the measured shifts by mediation of the hyperfine interactions with farther-out Co ions. These effects, which are not known to precision, are smaller than the primary hyperfine interaction by at least two orders of magnitude.[7] The random configuration beyond the first shell thus causes an inhomogeneous broadening of the resonances, rather than a further separation. Irrespective of the occupation of further shells, therefore, we refer to *all* local configurations about a central magnetic ion with n magnetic nearest neighbors as "n cluster." As for the identification with n, the resonances have, within errors, identical relaxation rates, and their integrated weights thus are expected to equal the binomial distribution $W_I(n)=[4!/n!(4-n)!]x^n(1-x)^{4-n}$. For $n=4$, 3, and 2, then, good agreement is achieved when the nominal $x=0.83\pm 0.01$ from atomic absorption is inserted (cf. Table I). For $x=0.83$, $n=1$ clusters are so infrequent as to escape observation in the present experiment [$W_I(1)=0.016$]. A further justification for the assignment is found in the development of the NMR frequencies with temperature to be discussed below. Analogously, the two close-lying $^{19}F_{II}$ resonances observed (Fig. 1) are identified as belonging to $^{19}F_{II}$ located between neighboring Zn and Co ions in $n=2$ and 3 clusters, which configurations contribute to the NMR intensity in the ratio 0.615 to 1.

The NMR frequencies associated with the various n clusters in $K_2Co_{0.83}Zn_{0.17}F_4$ are presented in Fig. 3 ($^{19}F_I$) and Fig. 4 ($^{19}F_{II}$) as a function of the temperature. The data are, for each cluster, analyzed in terms of a model based on an n cluster embedded in a virtual-crystal host. The z components of the spins residing at the host sites are taken to follow Onsager's relation, i.e.,

$$M_{VC}(T)=\tfrac{1}{2}[1-\sinh^{-4}(J_{VC}/k_B T)]^{1/8} .$$

The Hamiltonian of the cluster then reads

$$\mathcal{H}=-2J\sum_{\delta=1}^{n} m_\delta m_0-6J'\sum_{\delta=1}^{n} m_\delta M_{VC}(T)+\lambda m_0 , \qquad (2)$$

in which δ runs over the n Co spins of the first shell ($n\leq 4$), J and J' denote exchange parameters, and λ is introduced to extract the magnetization at the central site. The spin quantum numbers m_0 and m_δ may take on the values $\pm\frac{1}{2}$. It is noted that the Hamiltonian Eq. (2) is of the simplest form in which at the central site the energy of the local excitations is not renormalized, yet the magnetization drops to zero at the Néel temperature of the host. Constructing the partition function Z, and calculating the central magnetization by use of

$$M_0(T)=-k_B T\left[\frac{\partial \log Z(\lambda)}{\partial\lambda}\right]_{\lambda=0} ,$$

we arrive at

$$M_{0,n}(T)=\frac{1}{2}\frac{\cosh^n(\xi)-\cosh^n(\eta)}{\cosh^n(\xi)+\cosh^n(\eta)} , \qquad (3)$$

in which

$$\xi=[6J'M_{VC}(T)+J]/2k_B T$$

and

TABLE I. Results of fitting Eq. (3) to the NMR data of $K_2Co_{0.83}Zn_{0.17}F_4$.

Cluster	$\lvert J\rvert/k_B$ (K)	ν_I ($T=0$)[a] (MHz)	ν_{II} ($T=0$)[a] (MHz)	$W_I^{expt}(n)$	$W_I^{calc}(n)$
$n=4$	90±3	189.33±0.13		0.48±0.01	0.47
$n=3$	91±3	184.78±0.13	59.98±0.08	0.39±0.01	0.39
$n=2$	95±5	178.8 ±0.8	57.54±0.08	0.13±0.01	0.12

[a]The zero-field zero-temperature frequencies are not corrected for the Van Vleck susceptibility.

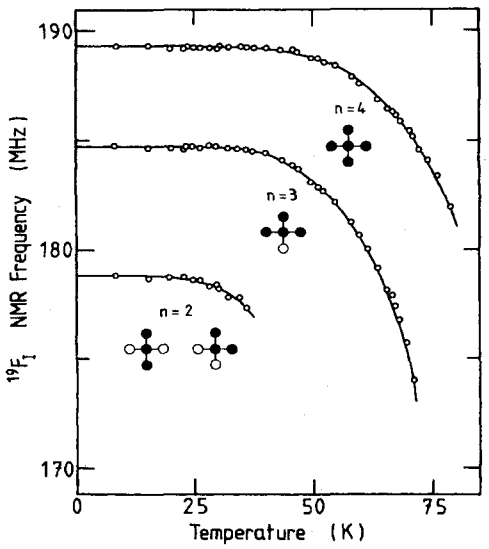

FIG. 3. Temperature dependence of the $^{19}F_I$-NMR frequencies, extrapolated to zero external field, for various n clusters in $K_2Co_{0.83}Zn_{0.17}F_4$, as indicated. Solid curves are according to the least-squares fit of Eq. (3) to the data.

$$\eta=[6J'M_{VC}(T)-J]/2k_BT\ .$$

In fitting Eq. (3) to the data of $K_2Co_{0.83}Zn_{0.17}F_4$, $M_0(T)$ for the various n is first derived from the measured NMR frequencies with account of the temperature dependence of A by the factor $1-(T/T_S)^4$. The exchange constant

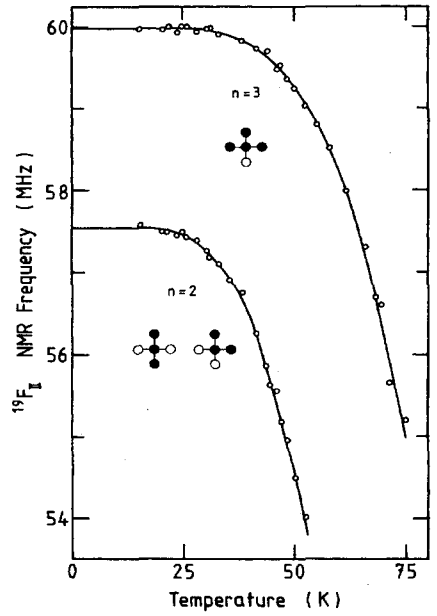

FIG. 4. Same as Fig. 3, but NMR of $^{19}F_{II}$ located between Co and Zn.

J_{VC} was set to -72.3 K, in conformity with $T_N=82$ K, determined independently from the uniform susceptibility [cf. Eq. (1)]. Excellent fits, represented by the solid curves in Figs. 3 and 4, were then obtained upon setting $J'=J$. The results for the zero-temperature zero-field frequencies and J, the latter averaged over the $^{19}F_I$ and $^{19}F_{II}$, are collected in Table I. For the sake of a comparison with the undiluted system, we have, inserting $J=J'=J_{VC}$ and $n=4$, also fitted Eq. (3) to the $^{19}F_I$ data of K_2CoF_4 up to 80 K to obtain $J/k_B=-92\pm3$ K, within errors equal to the fitted J of Eq. (1). The most significant finding of the analysis is that the output values of J associated with the various n clusters, $J(n)$, are close to J of pure K_2CoF_4. A similar conclusion was drawn with inelastic neutron scattering for $Rb_2Co_{0.7}Zn_{0.3}F_4$.[8] It was established that this system has four separate energy branches with only minor dispersion over the entire magnetic Brillouin zone. Most of the departure of $J(n)$ from J is presumably caused by lattice deformations. Upon substituting Zn for Co, the former having a 0.01 Å larger radius, the associated modifications of the exchange constants are estimated at several percent on the basis of an r^{-10} dependence. In connection with the $^{19}F_I$ data, we finally note that the further inhomogeneous broadening at higher temperatures appears to be in accord with a numerical partition-function calculation of the central magnetization of an n cluster in various configurations of the second shell. This calculation is an extension of the one above in that also the second shell is treated rigorously.

As to the $^{19}F_{II}$ nuclei located intermediate between two Co ions, their NMR spectrum consists of three distinct resonances, save a sharp line on top of the central resonance due to ^{19}F not neighboring any Co ion. The three resonances are separated at a distance of a few times their linewidth (FWHM 450 G). The peak positions relative to free ^{19}F are given in Fig. 5. The resonance line having a zero frequency shift at all temperatures is self-evidently associated with those $^{19}F_{II}$ that sense magnetizations of equal magnitude on the Co at either side, i.e., Co at the origins of clusters with equal n, notably $n=4$. The two other resonances, shifted beyond the linewidth, measure the balance of the magnetizations of neighboring Co ions centered in $n=4$ and $n=3$ clusters. The shifts are of about equal size, with the sign dependent on the sublattices. (Other combinations with $\Delta n=1$ contribute only weakly, while combinations with $\Delta n\geq2$ have escaped observation.) In Fig. 5, no corrections have been made for the minor asymmetry about zero related to the finite Van Vleck susceptibility. The asymmetry amounts to 0.1 MHz in external fields of about 10 kG, independent of the temperature. It is not feasible to make a detailed comparison with the experimental result $\chi_{VV}=3.5\times10^{-3}$ emu/mole (Ref. 9) because the relevant off-diagonal g factor is not known, but anyway the asymmetry estimated from χ_{VV} is of the order of the one observed. An interesting feature of the outer resonances is the rise of their shifts $\Delta\nu(T)$ above 40 K, quite directly indicating that the central magnetization of an $n=3$ cluster drops faster than that of an $n=4$ cluster. The shifts must, of course, vanish at $T_N=82$ K. An analysis of the observed shifts in terms of Eq. (3) is however, at best, qualitative, due to a

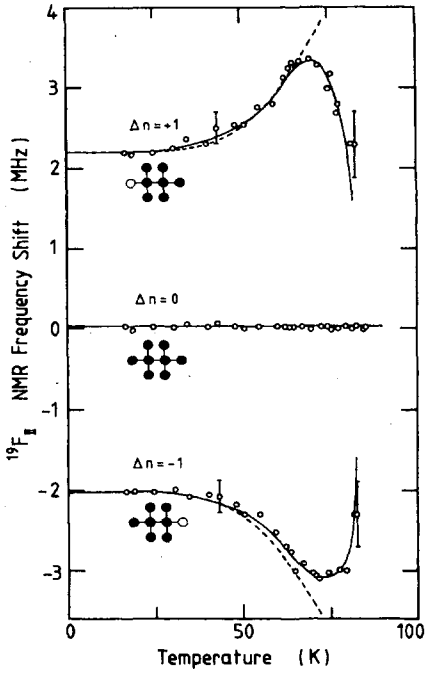

FIG. 5. Shift of the $^{19}F_{II}$-NMR frequency relative to free ^{19}F vs temperature in $K_2Co_{0.83}Zn_{0.17}F_4$. The external field, directed along the c axis, is about 10 kG. The clusters indicated are among those that contribute the most to the NMR intensities. Solid curves are guides to the eye. Dashed curves are calculated using Eqs. (3) and (4), with the parameters of Table I.

lack of precise knowledge of the relevant hyperfine constants as well as the contaminating hyperfine fields from further Co. Ignoring the second-neighbor hyperfine interactions, we have

$$\Delta\nu(T)=\pm[A_4M_{0,4}(T)-A_3M_{0,3}(T)]/h \ . \quad (4)$$

The approximative Eq. (4) with due correction for the field-induced asymmetry yields the dashed curves in Fig. 5, when adopting for A_3 and A_4 the hyperfine parameters of $^{19}F_{II}$ located between the central Co and Zn in $n=3$ clusters (≈ 120 MHz), however with allowance for a small difference such as to reproduce the observed shifts at low temperatures.

B. Heisenberg systems $K_2Ni_xZn_{1-x}F_4$

The NMR spectra of $K_2Ni_xZn_{1-x}F_4$ with $x=0.96$ and 0.85 show distinct resonances typically 600 G wide (FWHM). As in the case of the Co-based systems, these resonances are attributed to n clusters in such a way that their integrated weights within errors agree with the calculated $W(n)$. In Figs. 6 and 7 we present the $^{19}F_I$-NMR data for the average concentrations $x=0.96$ and 0.85, respectively. The data for these concentrations resemble one another to the extent that the spatial concentration fluctuations observed in these systems (Sec. II) have no bearing on the conclusions to be drawn below. The $n=2$ and 3 resonances cross at a temperature of about 25 K, while the $n=3$ and 4 resonances intersect near 50 K, complicating the determination of the various magnetizations

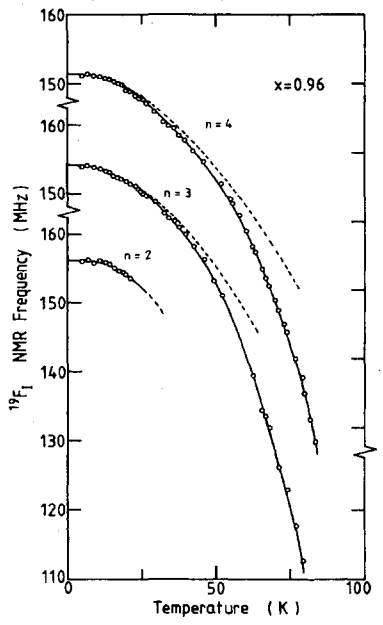

FIG. 6. Temperature dependence of the $^{19}F_I$-NMR frequencies for various n clusters in $K_2Ni_{0.96}Zn_{0.04}F_4$, extrapolated to zero external field. Solid curves are guides to the eye. Dashed curves are calculated using the Green's-function approach outlined in Sec. III B.

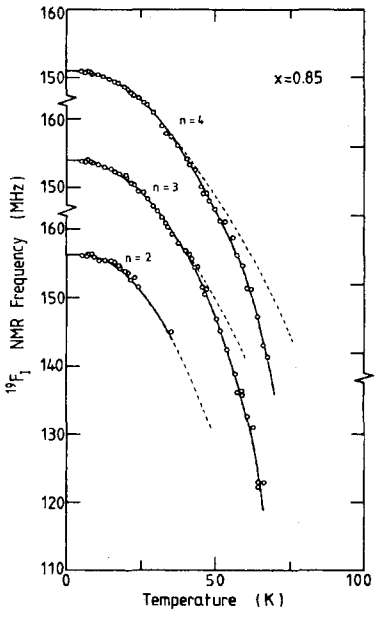

FIG. 7. Same as Fig. 6, but for $K_2Ni_{0.85}Zn_{0.15}F_4$.

at these temperatures. The results of $^{19}F_{II}$ NMR pertaining to the $x=0.85$ sample are given in Fig. 8. Already from a general inspection of the data one observes marked differences with the Ising case. First, the local magnetizations turn out to drop faster with temperature, as expected for diluted weakly anisotropic Heisenberg antiferromagnets. Second, and more relevant to the present study, the drops for the various n are to a first approximation congruent, indicating that the excitations causing the fall of the magnetization are delocalized to a substantial degree.

To calculate the temperature dependence of the magnetization residing at the central Ni ions of the various n clusters in $K_2Ni_xZn_{1-x}F_4$, we adopt the Green's-function formalism developed in Ref. 10. This theory is concerned with the local magnetization about isolated impurities embedded in a quadratic translation-invariant host. The perturbative Hamiltonian associated with the impurity is essentially restricted to a modification of the exchange between the impurity and the first shell of neighboring host spins. The spin-wave energies of the host system are supposed to be known. The magnetization residing at the impurity and the first shell about it are then recovered, at various temperatures, from the appropriate Green's functions in the energy domain. The Green's functions themselves have first been evaluated from their equations of motion, in which products of the local spin-deviation operators have been decoupled to quadratic within the random-phase approximation. The formalism has been worked out to deal with the effects on the first three shells, which is sufficient for the present purpose. In the present case, a K_2NiF_4-like virtual crystal is taken as the host system. To incorporate the dilution as far as the virtual crystal is concerned, the exchange constant is scaled down according to $T_N(x)$ with reference to pure K_2NiF_4.[11] That is, $J_{VC}=[T_N(x)/T_N(1)]J_{pure}$, in which $T_N(1)=97.23$ K (Ref. 4) and $J_{pure}/k_B=-102.1$ K.[3] In $K_2Ni_xZn_{1-x}F_4$, we have determined $T_N(x)$ with neutron diffraction[12] and susceptibility experiments, resulting in $T_N(0.96)=91.7$ K and $T_N(0.85)=76.5$ K. The associated modifications of the anisotropy parameter α have negligible effects, and accordingly we have kept α at the value 0.0021 appropriate to K_2NiF_4 (Ref. 3) throughout, leaving the exchange J_0 between the "impurity" and the first shell as the only parameter to be determined. A complete adjustment being quite arduous, we have considered a selection of reasonable forms of J_0 in terms of the other exchange parameters and n. We have chosen to compare with experiment $J_0=\frac{1}{4}nJ_{pure}$, $J_0=-\frac{1}{4}n(J_{VC}J_{pure})^{1/2}$, and $J_0=\frac{1}{4}nJ_{VC}$, noting that the exchange field at the central site will approximately scale with n whatever the effective exchange parameter. Out of these, the best results, given in Figs. 6–8 as the dashed curves, are produced by $J_0=\frac{1}{4}nJ_{VC}$. For all n the agreement is generally satisfactory up to temperatures of about $\frac{1}{2}T_N$, a point beyond which spin-wave-based theories for 2D antiferromagnets are known to fail.[3]

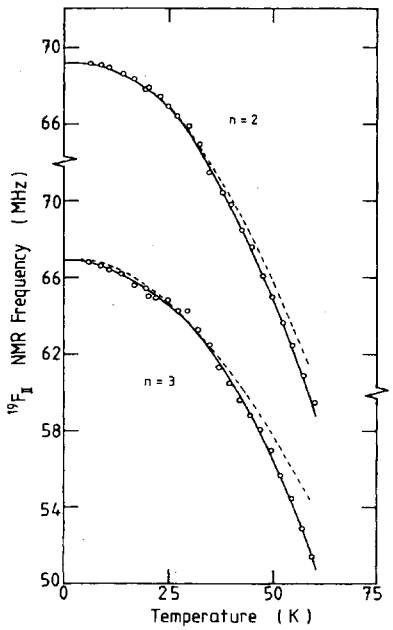

FIG. 8. Same as Fig. 6, but NMR of $^{19}F_{II}$ located between Ni and Zn in $K_2Ni_{0.85}Zn_{0.15}F_4$.

It is instructive to consider a few numerical results of the theory. First, it appears that n has no pronounced effects on the calculated magnetizations, in conformity with experiment. As a case in point, for $x=0.85$ at 40 K the calculated magnetization is, for $J_0=\frac{1}{4}nJ_{VC}$, thermally reduced by 0.066 units of spin at the central site of an $n=4$ cluster, by 0.074 units for $n=3$, and by 0.105 units for $n=2$. Second, the analysis indicates that the local magnetizations fall with temperature mainly because of spin-wave-like excitations just above the spin-wave gap, rather than excitations of local modes, excepting perhaps the case $n=1$. The gap occurs at an energy of $\epsilon=(2\alpha/R)^{1/2}=0.063$, expressed in units $4|J_{VC}|S$, with $R=1.079$ containing the spin-wave renormalization.[3] For $x=0.85$, the local modes appear, according to the calculations, to have the substantially higher reduced energies $\epsilon=0.97$, 0.67, 0.40, and 0.20 for $n=4$, 3, 2, and 1, respectively, compared to $n/4$ in Ising systems. These modes, heavily damped owing to coupling with the band, are confined to the disturbance, with small amplitudes at the first shell of neighbors.[13] These findings are supported by neutron scattering experiments on the comparable system $Rb_2Mn_{0.54}Mg_{0.46}F_4$ in that the dynamical response has a structure made up of four resonances fading near the zone center.[14] The localized modes, however, become not appreciably excited until a great number of long-wavelength excitations have already reduced the magnetizations.

To conclude this section, we present the results of an entirely different calculation, in which all lattice sites are treated equivalently. The calculation can only be conducted for lattices of limited size, yet lends support to the virtual-crystal approach in the sense that it confirms the energies of the modes localized at the clusters. The Hamiltonian used contains nearest-neighbor exchange of the Heisenberg form between the lattice sites occupied at random by Ni, augmented with a small staggered anisotropy

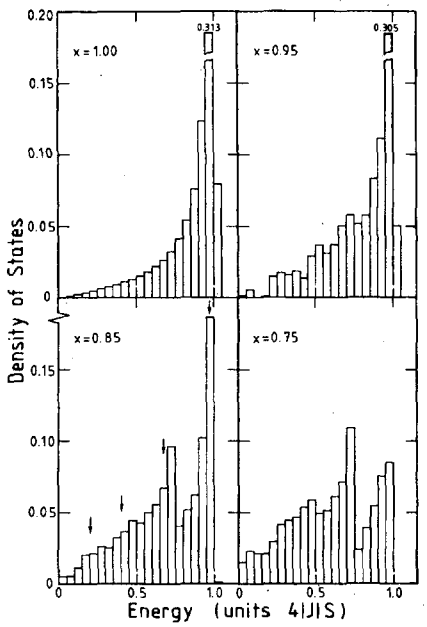

FIG. 9. Density of states vs the energy in units $4|J|S$ in $K_2Ni_xZn_{1-x}F_4$ for various x. Modes associated with Zn and isolated Ni ions, having zero energies, are removed. Resulting histograms are normalized to unit area. Arrows indicate the energies of the local modes calculated with Green's functions (Sec. III B) for the case $x=0.85$.

field stabilizing the spins perpendicular to the plane.[3] Following Holstein-Primakoff transformation, the coupled equations of motion of the local spin-deviation operators are solved numerically in the energy domain to first order in $1/2S$, yielding the energy spectrum of the excitations. The lattice is limited to a size of 16×16 sites, implying a dynamical matrix of dimension 256. Periodic boundary conditions are imposed. The resulting density of states $D(\epsilon)$ is presented in Fig. 9 for $x=0.95$, 0.85, and 0.75, in each case following averaging over 20 realizations of the random lattice. Figure 9 also contains the density of states of the pure system, for which an analytical expression is available,[13] here converted to a histogram with the same resolution as the computer results. An inspection of the evolution of $D(\epsilon)$ with x reveals, a shift toward lower energies aside, the development of a "resonance" at $\epsilon=0.7$, as well as weaker resonances near $\epsilon=0.4$ and 0.2. These energies compare well with the results $\epsilon=0.20$, 0.40, and 0.67 derived above with Green's functions for an impurity in a virtual crystal. The mode with $\epsilon=0.97$ is in the dynamical-matrix approach eclipsed by the high density of spin waves near the top of the band.

IV. CONCLUSIONS

Using NMR the magnetization at individual sites has been probed in the diluted 2D Ising-like antiferromagnet $K_2Co_xZn_{1-x}F_4$ and in the diluted Heisenberg antiferromagnet with weak anisotropy $K_2Ni_xZn_{1-x}F_4$. In $K_2Co_xZn_{1-x}F_4$, the fall with temperature of the magnetization at a particular ion depends almost exclusively on the number of Co ions n in its first shell of neighbors, which points to genuine localization of the relevant excitations. The associated excitation energies are close to $n|J|$. The marginal deviations from $n|J|$ are most likely caused by lattice deformations due to substitution of Zn for Co. The excitations of a Co surrounded by an incomplete shell therefore have energies below those of the band of the undiluted system. The appreciable spatial inhomogeneity of the local magnetization observed at finite temperatures is in full accord with an analytical expression derived with a simple partition-function calculation. Here, the exchange of the central ion with the Co ions occupying the first shell is treated explicitly, while the further shells are represented by a virtual-crystal host.

In $K_2Ni_xZn_{1-x}F_4$, by contrast, the drop of the magnetization shows only a weak n dependence, i.e., is close to uniform over the system. The drop is caused by low-lying collective excitations above the spin-wave energy gap rather than by excitations of local modes occurring at higher energies in the band. Good agreement is achieved between experiment and a Green's-function calculation based on a Ni impurity in a virtual-crystal host. The energies of the local modes calculated with this theory are confirmed by the results of a numerical diagonalization of the dynamical matrix pertaining to a 16×16 square lattice with the parameters appropriate to $K_2Ni_xZn_{1-x}F_4$ inserted.

ACKNOWLEDGMENTS

The authors acknowledge discussions with Dr. W. A. H. M. Vlak and technical assistance by C. R. de Kok. The electron-microscope analysis was performed by J. P. Pieters. This work was financially supported by the Netherlands Foundations Fundamenteel Onderzoek der Materie (FOM) and Zuiver Wetenschappelijk Onderzoek (ZWO).

[1]H. Ikeda and K. Hirakawa, Solid State Commun. **14**, 529 (1974).
[2]L. Onsager, Phys. Rev. **65**, 117 (1944).
[3]H. W. de Wijn, L. R. Walker, and R. E. Walstedt, Phys. Rev. B **8**, 285 (1973); **9**, 2419(E) (1974).
[4]R. J. Birgeneau, J. Als-Nielsen, and G. Shirane, Phys. Rev. B **16**, 280 (1977).
[5]K. N. Shrivastava, J. Phys. C **2**, 777 (1969).
[6]J. P. Gosso, P. Moch, M. Quilichini, J. Y. Gesland, and J. Nouet, J. Phys. (Paris) **40**, 1067 (1979).
[7]Supertransferred hyperfine-interaction constants have been determined in some iron-group-doped perovskite fluorides; R. K. Jeck and J. J. Krebs, Phys. Rev. B **5**, 1677 (1972).
[8]H. Ikeda and G. Shirane, J. Phys. Soc. Jpn. **46**, 30 (1979).
[9]D. J. Breed, K. Gilijamse, and A. R. Miedema, Physica **45**, 205 (1969).
[10]J. A. van Luijk, A. F. M. Arts, and H. W. de Wijn, Phys. Rev. B **21**, 1963 (1980).

[11]We have also examined a J_{VC} in which the random dilution is, on the average, stored in a prefactor x^2 to the exchange Hamiltonian of the *pure* system. The results are in conflict with the data for any reasonable J_0.
[12]B. J. Dikken, A. F. M. Arts, H. W. de Wijn, and J. K. Kjems, Phys. Rev. B **30**, 2970 (1984).
[13]H. van der Vlist, A. F. M. Arts, and H. W. de Wijn, Phys. Rev. B **30**, 5270 (1984).
[14]R. A. Cowley, G. Shirane, R. J. Birgeneau, and H. J. Guggenheim, Phys. Rev. B **15**, 4292 (1977).